**Supplementary Information**

InVEST model calculation and parameters

**1. Water yield**

The InVEST water yield model estimates water yield based on the principle of water balance. The rate of water yield reduction was used as Flood mitigation.

$$Y_{ij} = (1 - \frac{AET_i}{P_i}) \times P_i$$

Where $Y_{ij}$ (mm/yr) is annual water yield for pixel $i$ on land use/land cover (LULC) $j$ and, $AET_i$ (mm/yr) is actual annual evapotranspiration for pixel $i$ on LULC $j$ and $P_i$ (mm/yr) is annual precipitation for pixel $i$.

$$\frac{AET_i}{P_i} = 1 + \frac{PET_i}{P_i} - \left[1 + (\frac{PET_i}{P_i})^{\omega}\right]^{1/\omega}$$

where $PET_i$ is potential evapotranspiration and $\omega$ is a non-physical parameter that characterizes the natural climate-soil properties.

$$PET_i = K_{c,j} \times ET_{0,i}$$

where $ET_{0,i}$ is the reference evapotranspiration for pixel $i$ and $K_{c,j}$ is the vegetation evapotranspiration coefficient for pixel $i$ on LULC $j$. Reference evapotranspiration was calculated by Penman Monteith Equation.

$$\omega_i = Z \times \frac{AWC_i}{P_i} + 1.25$$

$$AWC_i = Min(Rest_layer_depth_i,\ Root_depth_i) \times PAWC_i$$

Where $\omega_i$ is a non-physical parameter that characterizes the natural climate-soil properties; $Z$ is a dimensionless constant, ranging from 1 to 30, that captures the local precipitation pattern and hydrogeological characteristics; $AWC_i$ (mm) is the volumetric

plant-available water content; $KC_{iJ}$ is the evapotranspiration coefficient for pixel $i$ on LULC $j$; $ET_{0,i}$ (mm/yr) is the reference evapotranspiration for pixel $i$; and $PAWC$ (mm) is the plant-available water capacity.

For non-vegetated LULC, the actual annual evapotranspiration is computed directly from the reference evapotranspiration and has an upper limit defined by the precipitation:

$$AET_{iJ} = Min\left(K_{ij} \times ET_{0_i}, P_i\right)$$

where $K_{ij}$ is the evapotranspiration coefficient for pixel $i$ on LULC $j$; $ET_{0_i}$ (mm/yr) is the reference evapotranspiration for pixel $i$ and $P_i$ (mm/yr) is the annual precipitation for pixel $i$.

**2 Soil conservation**

SC was evaluated by the RUSLE. The formula is as follows:

$$SR = R \times K \times LS \times (1 - C \times P)$$

Where: $R$, $K$ $LS$, $C$, and $P$ are the precipitation erosivity factor, soil erodibility factor, slope length and slope factor, vegetation cover factor, and management measures factor, respectively.

$$R = 1.735 \times 10^{\left(1.50 \times \log \sum_1^{12} \frac{P_i^2}{P} - 0.8188\right)}$$

where $R$ is the rainfall erosivity factor, MJ·mm·ha$^{-1}$·h$^{-1}$·yr$^{-1}$; $P$ is the annual precipitation, mm; and $P_i$ is the precipitation in month $i$, mm.

EPIC was used to calculate K, which has been successfully applied to northeast China (Ouyang et al., 2016):

$$K = \left\{0.2 + 0.3exp\left[-0.0256 \times sand\left(1 - \frac{silt}{100}\right)\right]\right\} \times \left(\frac{silt}{clay + silt}\right)^{0.3}$$

$$\times \left[1 - \frac{0.25soc}{soc + exp(3.72 - 2.95soc)}\right]$$

$$\times \left[1 - \frac{0.7sni}{sni + exp(-5.51 + 22.9sni)}\right]$$

$$sni = 1 - \frac{sand}{100}$$

where $sand$ is the sand content (%), $silt$ is the silt content (%), $clay$ is the clay content (%), and $soc$ is the SOC content (%).

This study adopts the LS calculation method proposed by Wang et al. (2022) that is suitable for China:

$$L = \left(\frac{\lambda}{22.1}\right)^m$$

$$m = \begin{cases} 0.2, & \theta \leq 1° \\ 0.3, & 1° < \theta \leq 3° \\ 0.4, & 3° < \theta \leq 5° \\ 0.5, & \theta > 5° \end{cases}$$

$$S = \begin{cases} 10.8\sin\theta + 0.03, & \theta < 5° \\ 16.8\sin\theta - 0.5, & 5° \leq \theta < 10° \\ 21.9\sin\theta - 0.96, & \theta \geq 10° \end{cases}$$

where $\lambda$ is the slope length (m) and $\theta$ is the slope gradient (°).

C and P are closely related to LULC types. Considering the purpose of this study, the corresponding C and P values are obtained by referring to previous study on BSR, which have been verified to be applicable (Fang and Fan, 2020; Wan et al., 2022). C and P values were shown in Table S2.

**3 Carbon storage**

Using maps of land use and land cover types, and data on the amount of carbon stored

in carbon pools, this model estimates the net amount of carbon stored in a land parcel over time as:

$$C_{total} = C_{above} + C_{below} + C_{soil} + C_{dead}$$

where $C_{total}$ is the total amount (Mg/ha) of carbon storage; and $C_{above}$, $C_{below}$, $C_{soil}$, and $C_{dead}$ represents the amount (Mg/ha) of carbon stored in aboveground biomass, belowground biomass, soil, and dead organic matter, respectively. Carbon pool data came from forest survey data.

**Model validation**

GP was calculated from validated open remote sensing products and statistical almanacs, and CS was calculated from validated LULC and reference previous studies' carbon density data. Thus, we only need to verify WY and SC. We used annual average water resources data to validate WY from the Heilongjiang, Jilin, Liaoning and Inner Mongolia Water Resources Bulletins. The result showed that the simulated WY was consistent with the observed WY ($R^2$=0.7681) (Fig. S1). The measured sediment yield at the outlet is often used to verify the accuracy of the soil erosion estimation at the watershed scale. However, eroded soil under the impacts of scouring, transport, deposition, and re-transport finally passes through the watershed outlet with runoff, leading to a sediment yield that is usually less than the amount of soil erosion. That is, the soil erosion is not equal to the soil transport of the watershed outlet in quantity, and there is a conversion coefficient (i.e., sediment delivery ratio, SDR) between soil erosion and soil transport. The parameter of SDR, calculated as sediment transport divided by soil erosion. As the SDR varies with different geomorphologic landscapes, the SDR of the rolling hilly and hilly-gully regions in Northeast China is 0.17570 and 0.03636, respectively, according to the long time series

monitoring results reported by Wang et al. (2013). The accuracy of soil erosion in Northeast China was verified using the China River Sediment Bulletin from the Ministry of Water Resources of the People's Republic of China (http://www.mwr.gov.cn/ ). The results showed that the modeled values and observed values for RUSLE showed a perfect linear regression, with $R^2$ values of 0.8158 (Fig. S2).

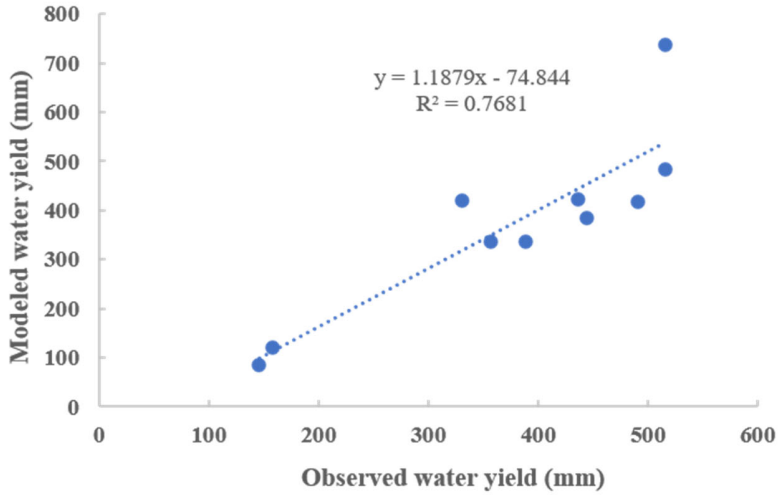



Figure S1. The observed data versus modeled data. Validation of water yield against data reported by Water Resources Bulletin.

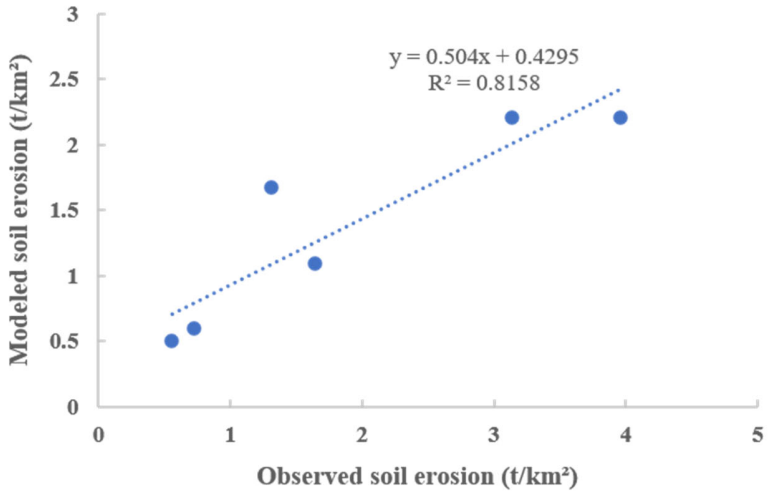



Figure S2. The observed data versus modeled data. Validation of RUSLE against data reported by China River Sediment Bulletin.

**Table S1.** Summary of the primary data.

| Data | Type | Spatial Resolution | Data source | Related model |
|---|---|---|---|---|
| Digital Elevation Model (DEM) | Raster | 30m×30m | Geospatial data cloud http://www.gscloud.cn/ | SC |
| Annual average precipitation | Raster | 1km×1km | National Tibetan Plateau Data Center http://data.tpdc.ac.cn | WY, SC |
| Reference evapotranspiration | Raster | 1km×1km | National Tibetan Plateau Data Center http://data.tpdc.ac.cn | WY |
| Plant-available water content | Raster | 1km×1km | Calculated by soil data http://data.tpdc.ac.cn | WY |
| Land use/land cover (LULC) | Raster | 30m×30m | Annual land cover datasets in China from 1990 to 2020 https://zenodo.org/record/5210928 | GP, WY, SC, CS, SED |

| | | | | |
|---|---|---|---|---|
| Maximum soil depth | Raster | 1km×1km | Calculated by soil datahttp://data.tpdc.ac.cn | WY |
| Normalized Difference Vegetation Index (NDVI) | Raster | 1km×1km | MOD13A2 https://modis.gsfc.nasa.gov/data/dataprod/mod13.php | GP |
| Watersheds | Shapefile | | Divided by DEM in ArcGIS 10.4 | WY |
| Biophysical data | .CSV file | | Literature and the InVEST user's guide (Sharp, et al., 2015). | WY, CS |
| Fractional Vegetation Cover (FVC) | Raster | 250m×250m | National Tibetan Plateau Data Center http://data.tpdc.ac.cn | SED |
| Gross Domestic Product (GDP) | Raster | 1km×1km | Resource and Environment Science and Data Center http://www.resdc.cn/ | SED |
| Population Density (POP) | Raster | 1km×1km | The World Pop Dataset https://www.worldpop.org/ | SED |

Note: GP: grain production; WY: water yield; SC: soil retention; CS: carbon storage; SED: social-ecological drivers.

**Table S2.** Critical parameter settings.

| LULC | Kc | root_depth | LULC_veg | C | P | C_above | C_below | C_soil | C_dead |
|---|---|---|---|---|---|---|---|---|---|
| Cropland | 1.2 | 700 | 1 | 0.228 | 0.325 | 4.7 | 0 | 33.46 | 0 |
| Forest land | 1 | 7000 | 1 | 0.004 | 1 | 51.87 | 34.1 | 166.26 | 2.21 |
| Grassland | 0.5 | 500 | 1 | 0.043 | 1 | 3.37 | 7.48 | 44.36 | 55 |
| Water body | 1 | 100 | 0 | 0 | 0 | 2.77 | 0 | 60.56 | 0 |
| Bare land | 0.1 | 10 | 0 | 1 | 1 | 0 | 0 | 0 | 0 |
| Built-up land | 0.1 | 10 | 0 | 0.03 | 1 | 0 | 0 | 0 | 0 |

Note: Kc: the plant evapotranspiration coefficient for each LULC class; root_depth: the maximum root depth for vegetated LULC classes in mm; C: the vegetation cover and management factor; P: the support practice factor; LULC_vegetation: a flag to distinguish bare land from vegetated land, 1 for vegetated land and 0 for others; C_above: carbon storage in aboveground biomass; C_below: carbon storage in belowground biomass; C_soil: carbon storage in soil; C_dead: carbon storage in dead organic matter.

**Table S3.** Comparison of the fitting measures for different models.

| | | | GP-WY | GP-SC | GP-CS | WY-SC | WY-CS | SC-CS |
|---|---|---|---|---|---|---|---|---|
| Pixel scale | OLS | $R^2$ | 0.32 | 0.30 | 0.20 | 0.14 | 0.12 | 0.12 |
| | | AICc | -411870 | -389109 | -300590 | -645469 | -311340 | -265361 |
| | GWR | $R^2$ | 0.73 | 0.73 | 0.49 | 0.44 | 0.39 | 0.35 |
| | | AICc | -522542 | -490266 | -335734 | -690681 | -350544 | -286818 |
| County scale | OLS | $R^2$ | 0.15 | 0.38 | 0.20 | 0.45 | 0.34 | 0.53 |
| | | AICc | -1159.03 | -550.747 | -1110.37 | -642.84 | -1629.3 | -630.046 |
| | GWR | $R^2$ | 0.35 | 0.76 | 0.37 | 0.77 | 0.58 | 0.82 |
| | | AICc | -1188.95 | -766.59 | -1128.12 | -850.134 | -1719.92 | -853.5 |

**Table S4.** proportion of positive and negative effects of drivers on the interactions between ES of different ERPs at different scales (%).

| | Scale | Effect | GFGP | | | | | LASP | | | | | NFCP | | | | | NWCP | | | | | TNSP | | | | |
|---|---|---|---|---|---|---|---|---|---|---|---|---|---|---|---|---|---|---|---|---|---|---|---|---|---|---|---|
| | | | CRP | FRT | SHDI | SL | FVC | CRP | FRT | SHDI | SL | FVC | CRP | FRT | SHDI | SL | FVC | CRP | FRT | SHDI | SL | FVC | CRP | FRT | SHDI | SL | FVC |
| GP-WY | Pixel | Positive | 62 | 78 | 40 | 52 | 47 | 26 | 72 | 19 | 38 | 42 | 70 | 77 | 46 | 50 | 56 | 84 | 89 | 44 | 64 | 67 | 40 | 73 | 38 | 51 | 32 |
| | | Negative | 38 | 22 | 60 | 48 | 53 | 74 | 28 | 81 | 62 | 58 | 30 | 23 | 54 | 50 | 44 | 16 | 11 | 56 | 36 | 33 | 60 | 27 | 62 | 49 | 68 |
| | County | Positive | 54 | 58 | 83 | 24 | 70 | 0 | 100 | 100 | 0 | 100 | 33 | 47 | 100 | 2 | 87 | 0 | 0 | 100 | 0 | 100 | 43 | 75 | 62 | 37 | 62 |
| | | Negative | 46 | 42 | 17 | 76 | 30 | 100 | 0 | 0 | 100 | 0 | 67 | 53 | 0 | 98 | 13 | 100 | 100 | 0 | 100 | 0 | 57 | 25 | 38 | 63 | 38 |
| GP-SC | Pixel | Positive | 61 | 76 | 46 | 52 | 43 | 36 | 74 | 20 | 40 | 43 | 70 | 78 | 55 | 48 | 51 | 82 | 88 | 58 | 57 | 63 | 69 | 74 | 24 | 68 | 60 |
| | | Negative | 39 | 24 | 54 | 48 | 57 | 64 | 26 | 80 | 60 | 57 | 30 | 22 | 45 | 52 | 49 | 18 | 12 | 42 | 43 | 37 | 31 | 26 | 76 | 32 | 40 |
| | County | Positive | 62 | 61 | 95 | 4 | 47 | 0 | 0 | 100 | 0 | 100 | 50 | 68 | 82 | 0 | 55 | 35 | 80 | 100 | 0 | 98 | 72 | 45 | 100 | 11 | 34 |
| | | Negative | 38 | 39 | 5 | 96 | 53 | 100 | 100 | 0 | 100 | 0 | 50 | 32 | 18 | 100 | 45 | 65 | 20 | 0 | 100 | 3 | 28 | 55 | 0 | 89 | 66 |
| GP-CS | Pixel | Positive | 37 | 38 | 26 | 59 | 43 | 50 | 42 | 23 | 35 | 37 | 28 | 43 | 24 | 65 | 50 | 58 | 34 | 21 | 65 | 45 | 43 | 36 | 32 | 56 | 33 |
| | | Negative | 63 | 62 | 74 | 41 | 57 | 50 | 58 | 77 | 65 | 63 | 72 | 57 | 76 | 35 | 50 | 42 | 66 | 79 | 35 | 55 | 57 | 64 | 68 | 44 | 67 |
| | County | Positive | 54 | 78 | 68 | 4 | 54 | 0 | 100 | 100 | 0 | 100 | 20 | 55 | 100 | 8 | 82 | 0 | 0 | 100 | 0 | 100 | 51 | 100 | 55 | 2 | 57 |
| | | Negative | 46 | 22 | 32 | 96 | 46 | 100 | 0 | 0 | 100 | 0 | 80 | 45 | 0 | 92 | 18 | 100 | 100 | 0 | 100 | 0 | 49 | 0 | 45 | 98 | 43 |
| WY-SC | Pixel | Positive | 69 | 73 | 24 | 74 | 60 | 94 | 70 | 34 | 69 | 76 | 56 | 63 | 28 | 79 | 56 | 83 | 84 | 12 | 68 | 63 | 69 | 74 | 24 | 68 | 60 |
| | | Negative | 31 | 27 | 76 | 26 | 40 | 6 | 30 | 66 | 31 | 24 | 44 | 37 | 72 | 21 | 44 | 17 | 16 | 88 | 32 | 37 | 31 | 26 | 76 | 32 | 40 |
| | County | Positive | 64 | 66 | 89 | 0 | 50 | 0 | 0 | 100 | 0 | 100 | 62 | 78 | 70 | 0 | 40 | 100 | 100 | 98 | 0 | 0 | 60 | 36 | 93 | 0 | 63 |
| | | Negative | 36 | 34 | 11 | 100 | 50 | 100 | 100 | 0 | 100 | 0 | 38 | 22 | 30 | 100 | 60 | 0 | 0 | 3 | 100 | 100 | 40 | 64 | 7 | 100 | 37 |
| WY-CS | Pixel | Positive | 44 | 30 | 24 | 65 | 49 | 97 | 43 | 31 | 56 | 53 | 25 | 34 | 25 | 71 | 50 | 51 | 20 | 19 | 64 | 45 | 62 | 28 | 29 | 64 | 49 |
| | | Negative | 56 | 70 | 76 | 35 | 51 | 3 | 57 | 69 | 44 | 47 | 75 | 66 | 75 | 29 | 50 | 49 | 80 | 81 | 36 | 55 | 38 | 72 | 71 | 36 | 51 |
| | County | Positive | 34 | 33 | 100 | 39 | 66 | 0 | 0 | 100 | 0 | 100 | 62 | 78 | 70 | 0 | 40 | 100 | 100 | 100 | 0 | 0 | 22 | 20 | 100 | 46 | 76 |
| | | Negative | 66 | 67 | 0 | 61 | 34 | 100 | 100 | 0 | 100 | 0 | 38 | 22 | 30 | 100 | 60 | 0 | 0 | 0 | 100 | 100 | 78 | 80 | 0 | 54 | 24 |
| SC-CS | Pixel | Positive | 43 | 32 | 23 | 64 | 48 | 96 | 44 | 31 | 59 | 46 | 22 | 35 | 24 | 71 | 49 | 53 | 21 | 17 | 66 | 37 | 60 | 32 | 28 | 64 | 49 |
| | | Negative | 57 | 68 | 77 | 36 | 52 | 4 | 56 | 69 | 41 | 54 | 78 | 65 | 76 | 29 | 51 | 47 | 79 | 83 | 34 | 63 | 40 | 68 | 72 | 36 | 51 |
| | County | Positive | 62 | 61 | 82 | 0 | 38 | 0 | 0 | 100 | 0 | 100 | 60 | 65 | 58 | 0 | 37 | 98 | 100 | 100 | 0 | 0 | 54 | 30 | 74 | 0 | 51 |
| | | Negative | 38 | 39 | 18 | 100 | 62 | 100 | 100 | 0 | 100 | 0 | 40 | 35 | 42 | 100 | 63 | 3 | 0 | 0 | 100 | 100 | 46 | 70 | 26 | 100 | 49 |

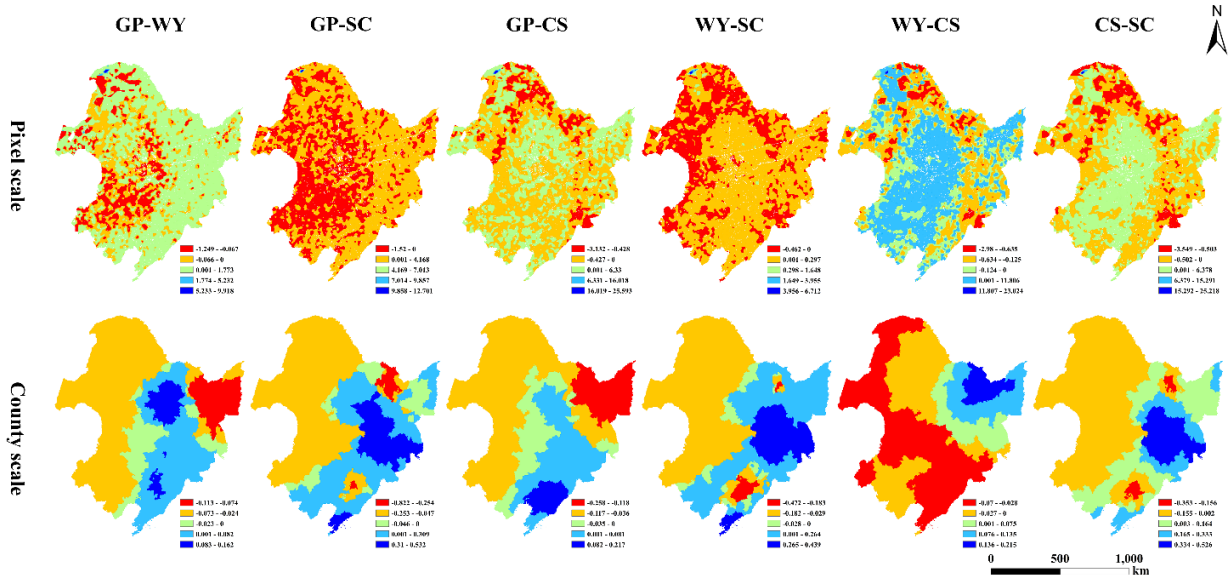



Figure S3. Spatial distribution of regression coefficients of CRP.

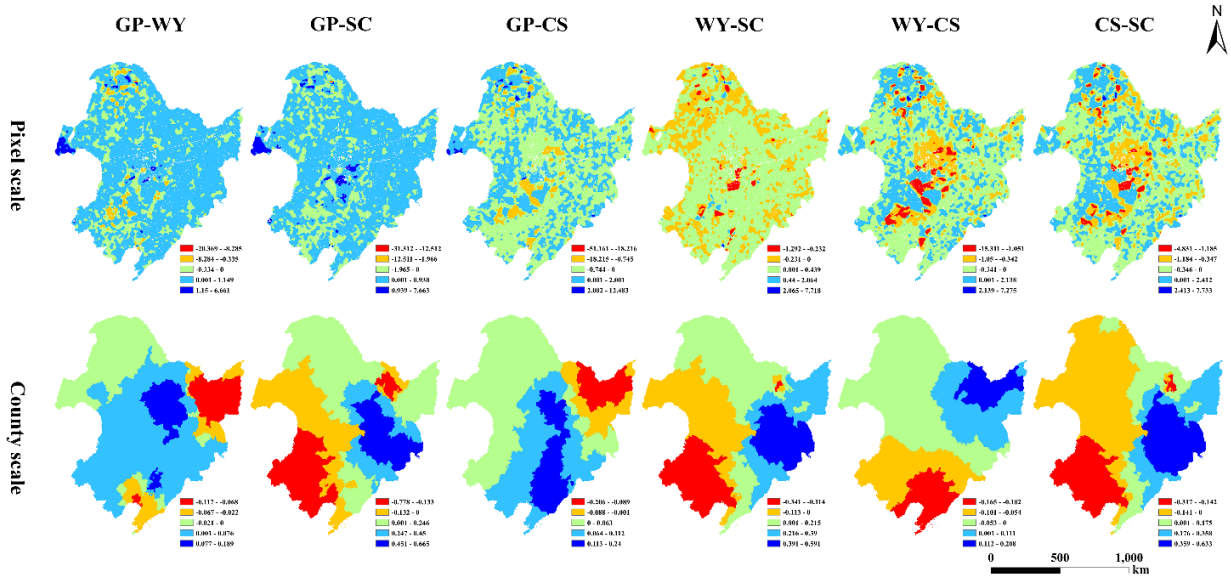



Figure S4. Spatial distribution of regression coefficients of FRT.

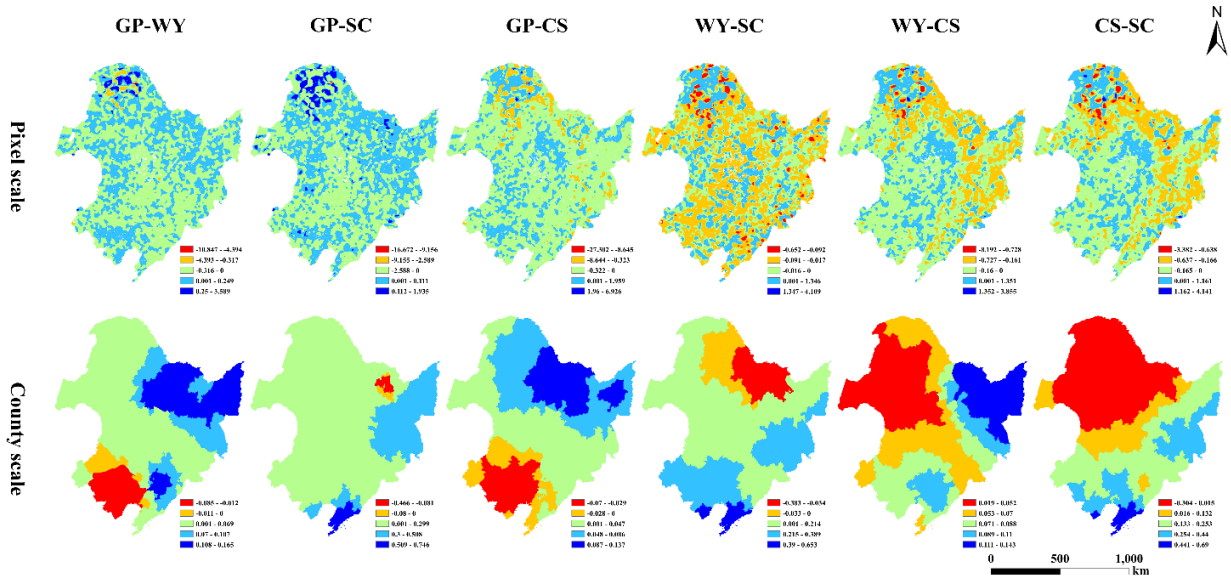



Figure S5. Spatial distribution of regression coefficients of SHDI.

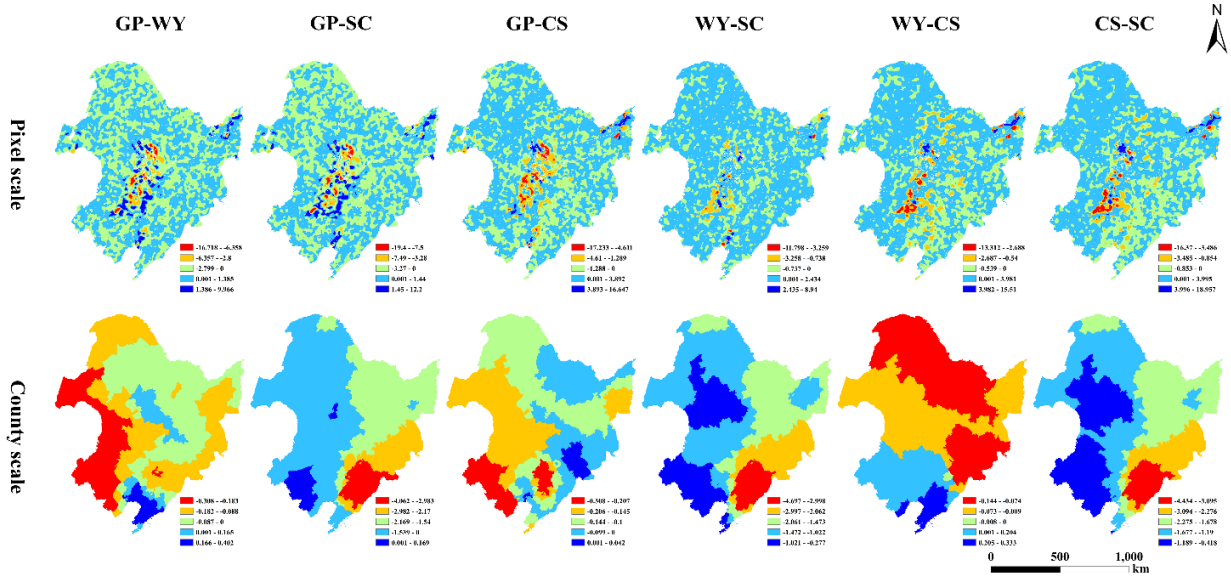



Figure S6. Spatial distribution of regression coefficients of SL.

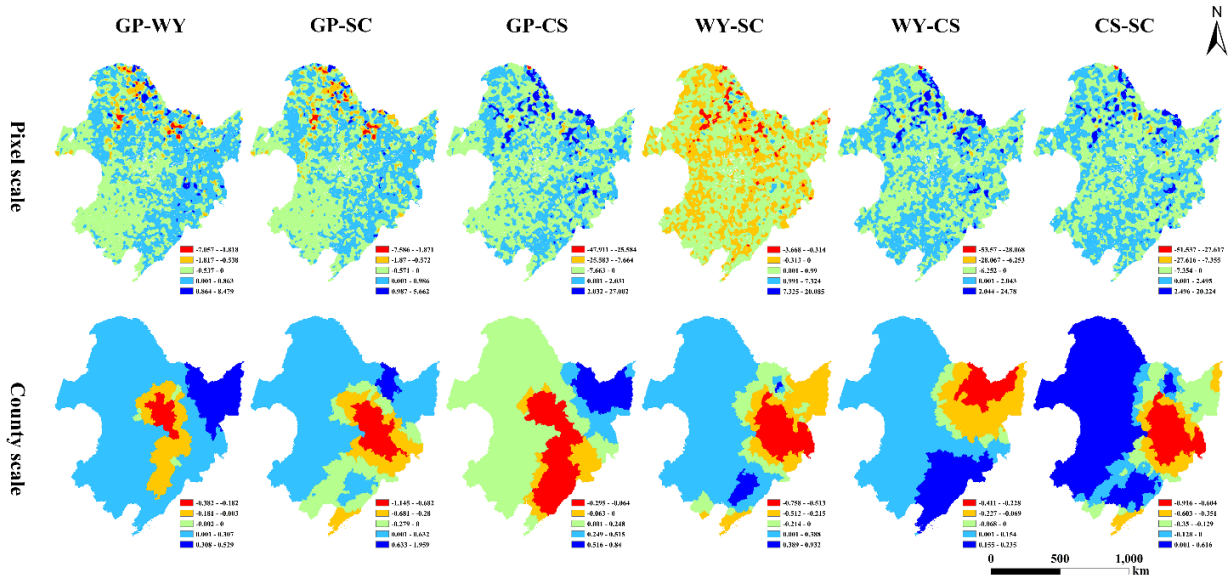



Figure S7. Spatial distribution of regression coefficients of FVC.

**References:**

Fang, H.; Fan, Z. Assessment of Soil Erosion at Multiple Spatial Scales Following Land Use Changes in 1980–2017 in the Black Soil Region, (NE) China. Int. J. Environ. Res. Public Health 2020, 17, 7378.

Ouyang, Z., Zheng, H., Xiao, Yi, Polasky, S., Liu, J., Xu, W., Wang, Q., Zhang, L., Xiao, Yang, Rao, E., Jiang, L., Lu, F., Wang, X., Yang, G., Gong, S., Wu, B., Zeng, Y., Yang, W., Daily, G.C., 2016. Improvements in ecosystem services from investments in natural capital. Science 352, 1455–1459.

Wan, W., Liu, Z., Li, B.G., Fang, H.Y., Wu, H.Q., Yang, H.Y., 2022. Evaluating soil erosion by introducing crop residue cover and anthropogenic disturbance intensity into cropland C-factor calculation: Novel estimations from a cropland-dominant region of Northeast China. Soil and Tillage Research 219, 105343.

Wang, Z., Jian, J., Jiao, J., Su, Y., 2013. Estimation of sediment delivery radio in different soil erosion regions in the Songhua River Basin based on RUSLE. Research of Soil and Water Conservation 20, 50-56.